

Article

Protective Role of Eicosapentaenoic and Docosahexaenoic and Their *N*-Ethanolamide Derivatives in Olfactory Glial Cells Affected by Lipopolysaccharide-Induced Neuroinflammation

Rosalia Pellitteri ^{1,*}, Valentina La Cognata ¹, Cristina Russo ², Angela Patti ^{3,*} and Claudia Sanfilippo ³

¹ Institute for Biomedical Research and Innovation, National Research Council, Via P. Gaifami 18, I-95126 Catania, Italy; valentina.lacognata@cnr.it

² Department of Biomedical and Biotechnological Sciences, Section of Pathology, University of Catania, Via Santa Sofia 97, I-95123 Catania, Italy; cristina.russo@unict.it

³ Institute of Biomolecular Chemistry, National Research Council, Via P. Gaifami 18, I-95126 Catania, Italy; claudia.sanfilippo@cnr.it

* Correspondence: rosalia.pellitteri@cnr.it (R.P.); angela.patti@cnr.it (A.P.)

Abstract: Neuroinflammation is a symptom of different neurodegenerative diseases, and growing interest is directed towards active drug development for the reduction of its negative effects. The anti-inflammatory activity of polyunsaturated fatty acids, eicosapentaenoic (EPA), docosahexaenoic (DHA), and their amide derivatives was largely investigated on some neural cells. Herein, we aimed to elucidate the protective role of both EPA and DHA and the corresponding *N*-ethanolamides EPA-EA and DHA-EA on neonatal mouse Olfactory Ensheathing Cells (OECs) after exposition to lipopolysaccharide (LPS)-induced neuroinflammation. To verify their anti-inflammatory effect and cell morphological features on OECs, the expression of IL-10 cytokine, and cytoskeletal proteins (vimentin and GFAP) was evaluated by immunocytochemical procedures. In addition, MTT assays, TUNEL, and mitochondrial health tests were carried out to assess their protective effects on OEC viability. Our results highlight a reduction in GFAP and vimentin expression in OECs exposed to LPS and treated with EPA or DHA or EPA-EA or DHA-EA in comparison with OECs exposed to LPS alone. We observed a protective role of EPA and DHA on cell morphology, while the amides EPA-EA and DHA-EA mainly exerted a superior anti-inflammatory effect compared to free acids.

Keywords: polyunsaturated fatty acids; *N*-eicosapentaenoyl ethanolamide; *N*-docosahexaenoyl ethanolamide; olfactory ensheathing cells; neuroinflammation; neuroprotection; neurodegenerative diseases

Citation: Pellitteri, R.; La Cognata, V.; Russo, C.; Patti, A.; Sanfilippo, C. Protective Role of Eicosapentaenoic and Docosahexaenoic and Their *N*-Ethanolamide Derivatives in Olfactory Glial Cells Affected by Lipopolysaccharide-Induced Neuroinflammation. *Molecules* **2024**, *29*, 4821. <https://doi.org/10.3390/molecules29204821>

Academic Editor: Pierluigi Plastina

Received: 3 September 2024

Revised: 2 October 2024

Accepted: 8 October 2024

Published: 11 October 2024



Copyright: © 2024 by the authors. Licensee MDPI, Basel, Switzerland. This article is an open access article distributed under the terms and conditions of the Creative Commons Attribution (CC BY) license (<https://creativecommons.org/licenses/by/4.0/>).

1. Introduction

Most degenerative diseases, such as Alzheimer's disease, Parkinson's disease, Huntington's disease, and multiple sclerosis, are associated with neuroinflammation, which is characterized by glia activation (microglia and astrocytes), resulting in the release of several soluble factors, including cytokines and chemokines [1,2]. These molecules are responsible for neuroinflammation and oxidative stress, two critical processes linked to neurodegenerative diseases. In addition, they are able to induce neurotoxicity and neurodegeneration and to alter neurotransmission [3,4]. The initial acute inflammation can turn into chronic, leading to tissue destruction and cell death caused by the macrophage and lymphocyte influx coming from the circulatory district, as observed in spinal cord lesions [5]. Guo et al. [6] reported that microglia, depending on micro-environmental modifications, may act both as pro-inflammatory and anti-inflammatory, inducing anti-inflammatory and neuroprotective effects. Indeed, pro-inflammatory microglia produce lactate, which promotes the release of cytokines and

interleukins [7,8], thus driving neuroinflammation, but on the other hand, it plays a role in resolving it and in repairing lesions of the nervous system [9].

In recent years, a growing interest has been directed towards the development of active drugs for the reduction or elimination of neuroinflammation effects, considered as symptoms in the onset of different neurodegenerative diseases. Eicosapentaenoic acid (EPA, 20:5, *n*-3) and docosahexaenoic acid (DHA, 22:6, *n*-3), belonging to the class of *n*-3 long-chain polyunsaturated fatty acids (PUFA), are known as important constituents (especially DHA) of brain phospholipids and play a critical role in the structure and functions of neuronal membranes [10,11]. In fact, the brain is the organ richest in lipids after adipose tissue [12]. A difference between EPA and DHA consists in their distribution in the brain: DHA is present at a high concentration within the brain compared with EPA, and both are able to cross the blood–brain barrier [13]. Some authors reported that when rat hippocampal culture medium was added with DHA, an increase in both neurite length and the number of neuronal branches was observed [11]. Other studies have highlighted that DHA stimulates the release of brain-derived neurotrophic factor (BDNF) and is able to control morphology and synaptogenesis [14,15], so acting as a potential therapeutic agent in neurodegenerative diseases [16]. These observations suggest an important relation between DHA deficit and the onset of neurodegenerative diseases [17].

A plethora of studies based on *n*-3 PUFA dietary supplementation have provided converging evidence that alterations in PUFA levels and metabolism may affect the control of neuroinflammation and related degenerative processes [18,19]. In vitro experiments on microglial cells exposed to lipopolysaccharide (LPS)-induced inflammation have evidenced that free *n*-3 PUFA displays dose-dependent anti-inflammatory activity, exerted by means of different mechanisms such as the inhibition of NO synthase and COX-2 inflammatory enzymes, the reduction in the expression of matrix metalloproteinase (MMP-9) and the decrease in the production of proinflammatory cytokines [20–22].

Through oxidative enzymatic pathways, PUFA is converted into specific derivatives, such as resolvins, protectins, and maresins, which have emerged as “specialized pro-resolving mediators (SPM)” of inflammation [23,24], while their conjugation with amines leads to PUFA-amides that exert their effects through interaction with cannabinoid receptors CB1 and CB2 [25]. Increased levels of docosahexaenoyl ethanolamide (DHA-EA) have been detected in the brains of animals fed with a DHA/EPA-supplemented diet, and its role in the suppression of neuroinflammation in mice has been related to the enhancement of cAMP/PKA signaling and the inhibition of NF- κ B activation [26].

In spite of mounting evidence of beneficial influences of *n*-3 PUFA and related derivatives, the elucidation and comparison of specific effects due to individual *n*-3 PUFA compounds is rather limited [13] and deserves focused investigation. In this context, we planned to individually test EPA and DHA, as well as the corresponding *N*-ethanolamides EPA-EA and DHA-EA, for their protective effect on Olfactory Ensheathing Cells (OECs) exposed to LPS-induced neuroinflammation.

OECs constitute an unusual population of glial cells present in the Olfactory System, sharing properties with both Schwann cells of the Peripheral Nervous System (PNS) and astrocytes of the Central Nervous System (CNS). They accompany the small nonmyelinated axons of the Olfactory Receptor Neurons along their whole length, from the basal lamina of the epithelium to the olfactory bulb, crossing the transitional zone between the PNS and CNS [27–29]. The OECs are a source of different growth factors [29–31], also expressing adhesion molecules [32] and numerous markers [29], including nestin [33], which is a specific stem cell marker. For their properties, they are able to stimulate axonal regeneration in the lesioned sites of the Nervous System, restoring functional connections and promoting vascularization and remyelination of damaged axons [34,35]. Another very important peculiarity of OECs consists in their ability to intermingle with astrocytes when transplanted, unlike Schwann Cells, which instead stimulate astrocytic gliosis and cystic cavitation in damaged sites [36]. Furthermore, many authors have

highlighted the phagocytic activity of OECs, which is useful for removing necrotic cells and stimulating neural regrowth [36,37], and it has been demonstrated that these cells are able to produce anti-inflammatory molecules regulating, when transplanted, inflammation localized in the injured spinal cord [38]. In addition, in a previous study, we have shown that OECs express ghrelin, a gut-brain peptide hormone with anti-inflammatory, antioxidant, and anti-apoptotic properties, and its receptor [39].

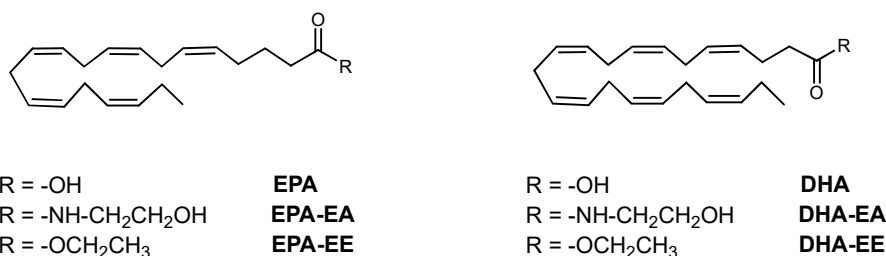
Therefore, contrasting neuroinflammation in OECs could offer a novel therapeutic target for neurological diseases, and we planned to investigate the potential protective role of EPA and DHA, as well as the corresponding *N*-ethanolamides EPA-EA and DHA-EA, for the first time in OECs. In all the experiments, both OECs alone and OECs exposed to LPS-induced neuroinflammation for 24 h were treated with the target compounds, while untreated OECs but LPS-stressed were used as a reference for the cytotoxic effects induced by inflammation. In the first instance, the treatment-induced changes in cell morphology and viability were assessed. Then, since apoptosis and mitochondrial dysfunctions play an important role in the physiological development of the nervous system, brain aging, and the onset and progression of several neurodegenerative diseases [40], mitochondrial toxicity and apoptosis levels were evaluated by specific tests (MitoHealth and TUNEL assays, respectively). Furthermore, the expression of some proteins, whose increased production is associated with neuroinflammation, was evaluated by immunocytochemical procedures. In this context, we considered IL-10, which is one among many cytokines produced by LPS induction, and Glial Fibrillary Acidic Protein (GFAP) and vimentin, two cytoskeleton markers indicating glial reactivity, as it is known that LPS is a glial activator for the inflammatory induction in neural cells with microglia activation [41].

Here, we report the obtained results that evidenced positive effects exerted by EPA, DHA, EPA-EA, and DHA-EA in contrasting neuroinflammation, in some cases with chemical structure-related differences.

2. Results

2.1. Chemical Compounds

While free acids, EPA and DHA, are commercially available, the corresponding amides were prepared by aminolysis of the ethyl esters of EPA and DHA with ethanolamine in the presence of immobilized lipase from *Candida antarctica* (Novozym 435) and molecular sieves in tert-butyl methyl ether. This biocatalyzed procedure offers advantages in mild reaction conditions and complete chemoselectivity toward the formation of amides over esters, resulting in a high yield of the target products EPA-EA and DHA-EA [42]. The amides were checked for their purity (>98%) by HPLC and ¹H-NMR analysis immediately before their dissolution in DMSO for biological assays (Scheme 1).



Scheme 1. Chemical structures of the compounds tested in this study and their synthetic precursors.

2.2. Morphological Features of OECs after Treatments

Our study was focused on exposing OECs to LPS to induce an inflammatory event. In physiological conditions, the majority of OECs exhibited both star and spindle shapes (Figure 1), which are typical morphological features of *in vitro* OECs [29,33].

To control morphological changes induced by the different treatments, the cells were monitored by phase-contrast inverted microscopy, and by this way, it was evidenced that EPA, DHA, and EPA-EA did not promote morphological variations at the tested concentrations, while DHA-EA at both concentrations caused some cell suffering and a reduction in cell number if compared with the controls (Figure 2A), as also observed following exposure to LPS.

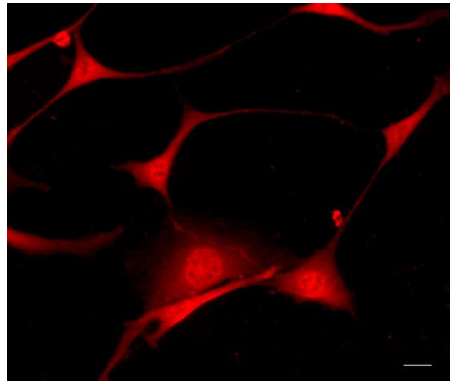


Figure 1. Immunofluorescent staining for S-100 protein expression in primary mouse OECs. Magnification: 20 \times . Scale bar: 10 μ m.

When OECs were exposed to LPS and treated with EPA or DHA, the examination of the cell morphological features revealed a protective effect at both tested concentrations. On the contrary, EPA-EA and DHA-EA protected LPS-exposed OECs only at higher concentrations, while at lower concentrations, it seemed that the cells lost their usual morphology (Figure 2B).

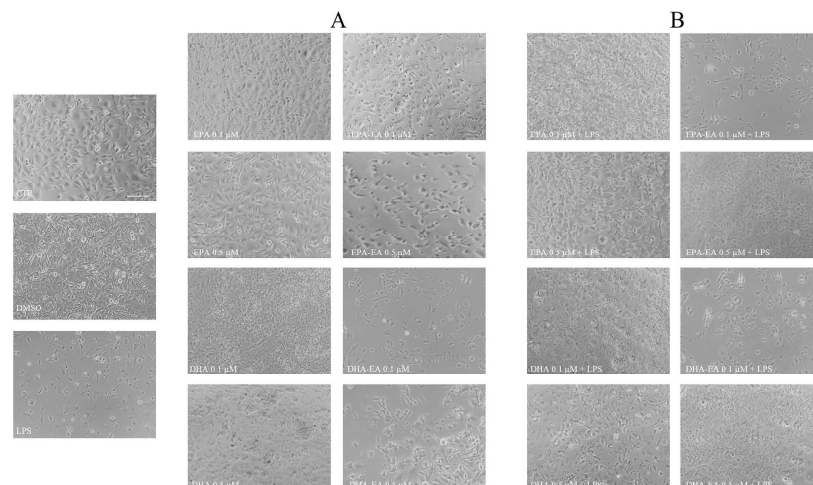


Figure 2. Morphological analysis of OECs by phase contrast microscopy. Representative fields of OECs, without (A) and with (B) LPS exposure, were treated with EPA, DHA, EPA-EA, and DHA-EA at different concentrations (0.1 μ M and 0.5 μ M) for 24 h. Magnification: 10 \times . Scale bars: 50 μ m.

2.3. Cell Viability (MTT Test)

In all experimental conditions, the MTT test was performed in order to evaluate the cell viability. The optimal concentrations of EPA, DHA, and the corresponding amides, as well as the suitable time of exposure, were chosen after a set of preliminary experiments. As shown in Figure 3, LPS was able to decrease the percentage of cell viability by almost 50% compared to control and DMSO, the latter used to solubilize the tested compounds. When the OECs were treated with EPA or DHA, better cell viability was determined at 0.1 μM for both molecules compared to 0.5 μM , and the treatment with EPA protected the LPS-exposed OECs more incisively than DHA in both the tested concentrations. Treatment with amides EPA-EA and DHA-EA decreased cell viability compared with the controls (CTR and DMSO), with a major incidence at 0.5 μM for EPA-EA and at 0.1 μM for DHA-EA. When OECs were exposed to LPS, the treatment with all the tested compounds resulted in sensibly higher cell viability compared to the control, and EPA at 0.1 μM concentration was the most effective. The treatment with DHA led to lower cell viability compared to EPA at both the tested concentrations, while EPA-EA and DHA-EA showed similar outcomes in protecting LPS-exposed OECs, with higher activity at 0.5 μM concentration. These data are comparable with those obtained by phase-contrast inverted microscopy.

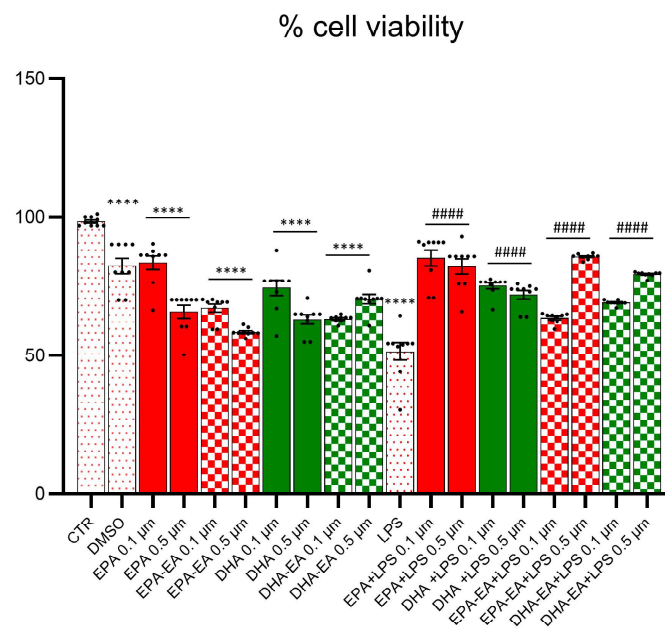


Figure 3. Percentage of viable OECs after treatment with EPA, DHA, EPA-EA, and DHA-EA. OECs without or with LPS stress were treated with EPA, DHA, EPA-EA, and DHA-EA at different concentrations (0.1 μM and 0.5 μM) for 24 h. One-way ANOVA experimental groups vs. CTR, $F(18, 152) = 37.60$. One-way ANOVA experimental groups vs. LPS, $F(16, 136) = 28.58$. Dunnett's multiple comparison test: **** $p < 0.0001$ vs. CTR; #### $p < 0.0001$ vs. LPS.

2.4. Influence on OEC Apoptosis (TUNEL Assay)

To evaluate the death of OECs exposed to LPS and treated with EPA or DHA, we used the TUNEL assay, based on the incorporation of modified nucleotide dUTPs by the enzyme terminal deoxynucleotidyl transferase (TdT) at the 3'-OH ends of fragmented DNA. The exposure to LPS for 24 h determined a significant increase in TUNEL-positive cells, denoting the presence of a higher amount of fragmented DNA and higher death levels if compared to controls (CTR and DMSO). The treatment with EPA and EPA-EA at

0.1 μM and DHA at both 0.1 μM and 0.5 μM did not cause significant changes in the number of dead cells compared to controls (Figure 4A,C). When OECs were exposed to LPS, the treatment with EPA or DHA in both concentrations reduced the levels of fragmented DNA, decreasing the number of TUNEL-positive cells. This result was more evident for LPS-exposed OECs treated with DHA at 0.1 μM concentration (Figure 4B,C).

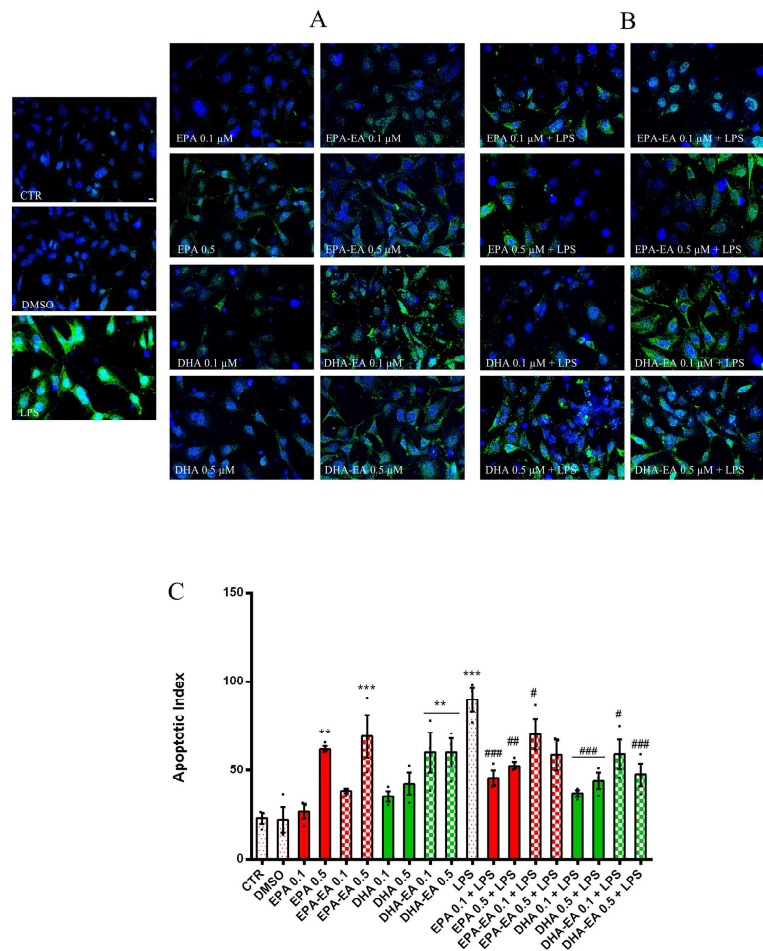


Figure 4. Dead cell detection by TUNEL assay. The test was carried out on OECs without (A) and with (B) LPS exposure and treated with EPA, DHA, EPA-EA, and DHA-EA. Photomicrographs are representative of randomly selected fields and were scanned by a Nikon Ti Eclipse inverted microscope. Scale bar 10 μm . (C) Data were taken from at least three independent experiments. TUNEL-positive cells were calculated as described in Section 4 and are reported as mean \pm SEM. One-way ANOVA experimental groups vs. CTRL condition $F(10, 22) = 9.913$; $p < 0.0001$; One-way ANOVA experimental groups vs. LPS treatment $F(8, 18) = 6.616$; $p = 0.0004$; Dunnett's multiple comparison tests: ** $p < 0.01$ and *** $p < 0.001$ vs. Ctrl; # $p < 0.05$, ## $p < 0.01$ and ### $p < 0.001$ vs. LPS.

2.5. Mitotoxicity and Cytotoxicity of LPS in OECs (MitoHealth Assay)

To investigate the protective effects of tested compounds in OECs exposed to LPS, we used a double-stain-based commercial kit able to simultaneously measure both mitotoxicity and cytotoxicity. In particular, the MitoHealth red stain accumulated in mitochondria in live cells proportionally to the mitochondrial membrane potential, and Image-iT® DEAD™ Green penetrates inside cells when plasma membrane integrity is compromised, so measuring the cytotoxicity. We found that incubation of OECs with LPS

determined a significant decrease in MitoHealth staining and an increase in DeadGreen accumulation against controls (Figure 5), as the exposed OECs exhibited lower mitochondrial membrane potential and reduced membrane integrity compared with controls. Our results show that LPS causes mitochondrial malfunction and the formation of green fluorescent nucleic acid aggregates at the nuclear level. The treatment of OECs with EPA (acids or amides) at 0.5 μM concentration and DHA-EA at both concentrations determined a significant activation of mitochondrial activity, which was maintained for EPA and DHA at 0.5 μM and DHA-EA at both concentrations (Figure 5A,C) also when cells were exposed to LPS (Figure 5B,C). The cytotoxicity evaluated by DeadGreen accumulation (Figure 5D) was in accordance with TUNEL results (Figure 4C).

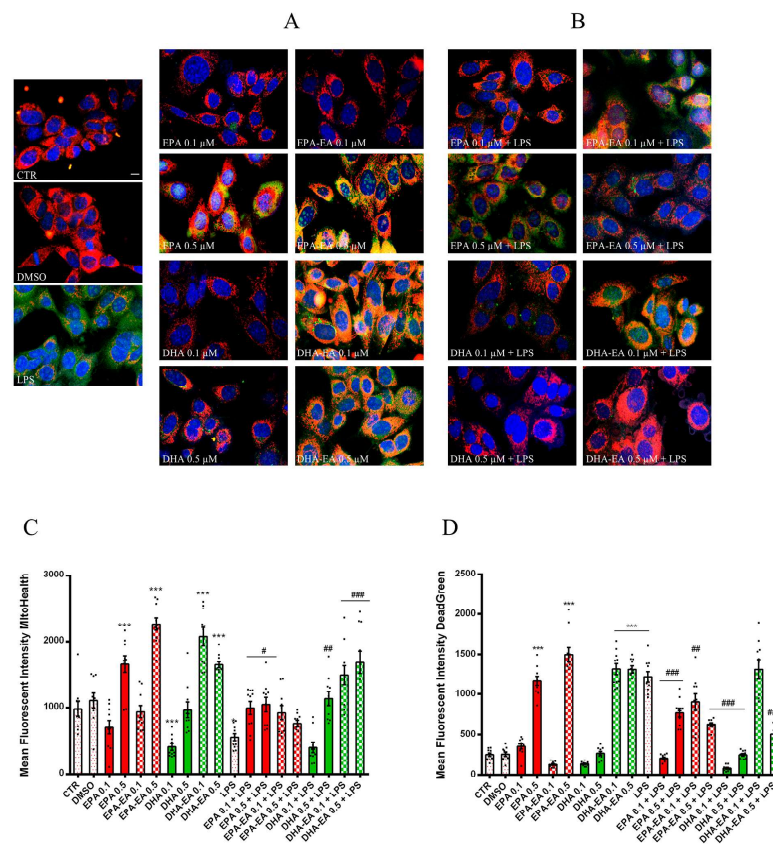


Figure 5. Mitotoxicity and cytotoxicity levels in OECs exposed to different treatments. The test was carried out on OECs without (A) and with (B) LPS exposure and treated with EPA, DHA, EPA-EA, and DHA-EA. Representative images were taken from randomly selected fields of slides scanned by a Nikon Ti Eclipse inverted microscope (scale bar 10 μm). Mean Fluorescent Intensity (MFI) values (mean \pm SEM) of the ratio MitoHealth (C) and DeadGreen (D) were calculated as described in the Material and Methods Section. Values are reported as mean \pm SEM. For Mitohealth staining, One-way ANOVA experimental groups vs. CTRL condition $F(10, 99) = 38.81$; $p < 0.0001$; One-way ANOVA experimental groups vs. LPS treatment $F(8, 81) = 14.69$; $p < 0.0001$. For DeadGreen staining, One-way ANOVA experimental groups vs. CTRL condition $F(10, 99) = 137.8$; $p < 0.0001$; One-way ANOVA experimental groups vs. LPS treatment $F(8, 81) = 49.71$; $p < 0.0001$. Dunnett's multiple comparison test: *** $p < 0.001$ vs. CTRL, # $p < 0.05$, ## $p < 0.01$, and ### $p < 0.001$ vs. LPS.

2.6. IL-10 Expression by Immunofluorescence

The expression of the anti-inflammatory marker IL-10 in the OECs grown in all the different conditions was evaluated through the immunofluorescence technique, and the

experimental model was effective in demonstrating that LPS was able to stimulate an inflammatory activity. The treatment of OECs with all the considered compounds did not give any strong evidence of inflammation (Figure 6A), even if a slightly enhanced positivity was revealed by the fluorescence quantification (Figure 6C). A strong positivity to IL-10 was found in OECs exposed to LPS, but in the presence of EPA, DHA, EPA-EA, and DHA-EA at both concentrations, the labeling sensibly decreased, indicating an active role of the tested compounds in protecting the cells from LPS-induced neurotoxic effects. (Figure 6B). More in detail, the fluorescence quantification (Figure 6C) evidenced that in the presence of EPA-EA or DHA-EA, the same levels of IL-10 expression as in control were found in OECs, both non-stressed and stressed with LPS.

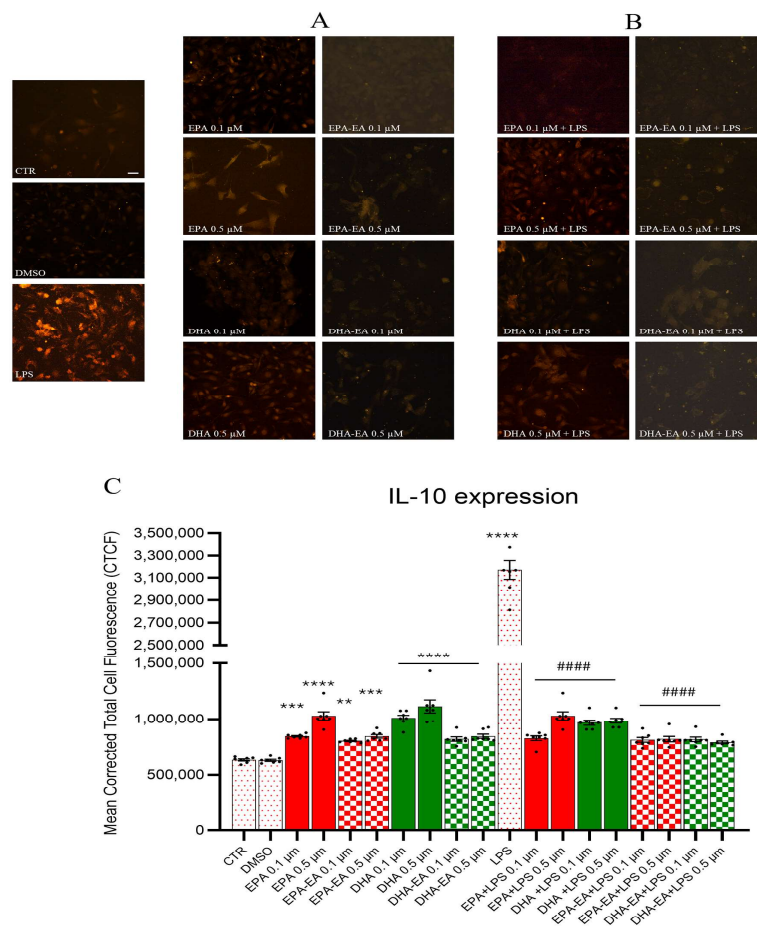


Figure 6. Immunocytochemistry for IL-10 in OECs exposed to different treatments. The test was carried out on OECs without (A) and with (B) LPS exposure and treated with EPA, DHA, EPA-EA, and DHA-EA. Immunostained samples were analyzed with a Zeiss fluorescence microscope, and images were captured with the Axiovision imaging system. (C) Fluorescence quantification data for IL-10 in each OEC cultured in different conditions. Bars represent CTCF mean value \pm SD, obtained from at least three independent experiments. One-way ANOVA experimental groups vs. LPS, $F(18,114) = 292.8$. One-way ANOVA experimental groups vs. LPS, $F(16, 102) = 278.5$. Dunnett's multiple comparison test: ** $p < 0.01$; *** $p < 0.001$; **** $p < 0.0001$ vs. CTR; #### $p < 0.0001$ vs. LPS. Scale bar 20 μ m.

2.7. GFAP and Vimentin Expression by Immunofluorescence

To identify glial reactivity in OECs and related changes in morphological features, the expression of some cytoskeleton markers, such as GFAP and vimentin, was evaluated

by immunocytochemistry in cells treated with EPA, DHA, EPA-EA, and DHA-EA at both concentrations (0.1 μM and 0.5 μM) and exposed or not to LPS.

As shown in the control samples of Figures 7 and 8, a strong positivity for both proteins, GFAP and vimentin, was found in OECs exposed to LPS with respect to controls, as the inflammatory activity induces the activation of the glia cells. The treatment of OECs with the tested compounds showed some increase in vimentin expression for EPA and DHA but not for EPA-EA and DHA-EA, as better evidenced by fluorescence quantification (Figure 7A,C). When the same test was carried out for the detection of GFAP expression, no substantial difference was found between EPA and DHA treatment compared to the non-treated OECs (Figure 8A,C).

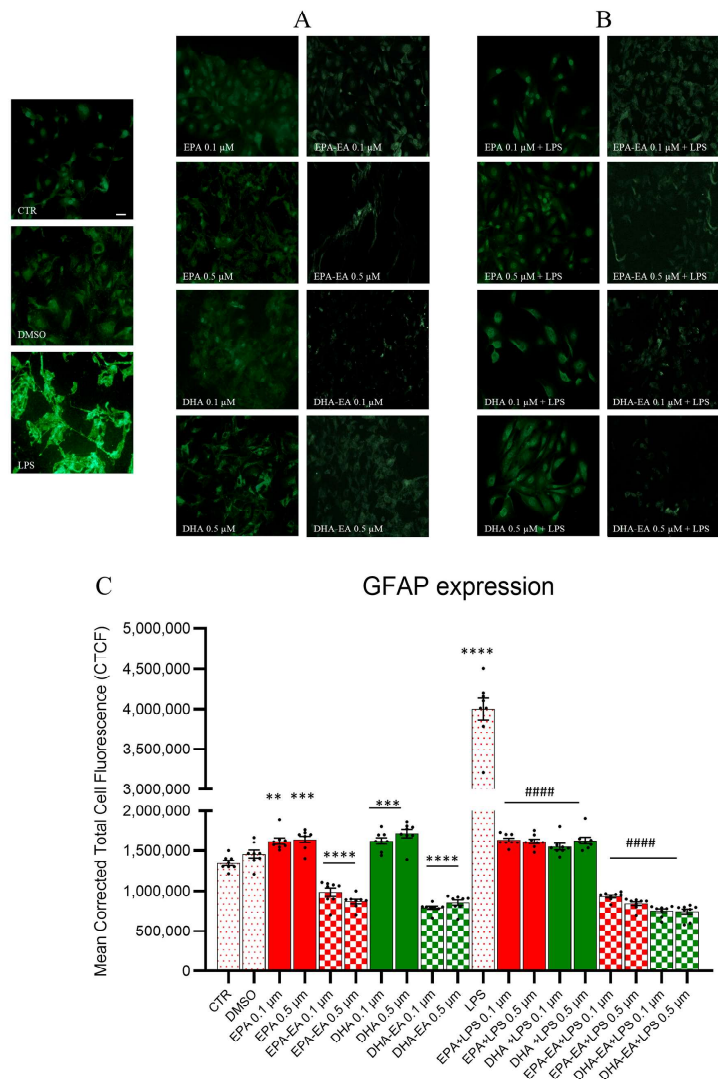


Figure 7. Immunocytochemistry for GFAP in OECs exposed to different treatments. The test was carried out on OECs without (A) and with (B) LPS exposure and treated with EPA, DHA, EPA-EA, and DHA-EA. (C) Fluorescence quantification data for GFAP in each OEC treatment with EPA, DHA, EPA-EA, and DHA-EA at different concentrations (0.1 μM and 0.5 μM). Bars represent CTCF mean value \pm SD, obtained from at least three independent experiments. One-way ANOVA experimental groups vs. CTR, $F(18, 133) = 101.5$. One-way ANOVA experimental groups vs. LPS, $F(16, 119) = 116.5$. Dunnett’s multiple comparison test: ** $p < 0.01$; *** $p < 0.001$; **** $p < 0.0001$ vs. CTR; #### $p < 0.0001$ vs. LPS. Scale bar 20 μm .

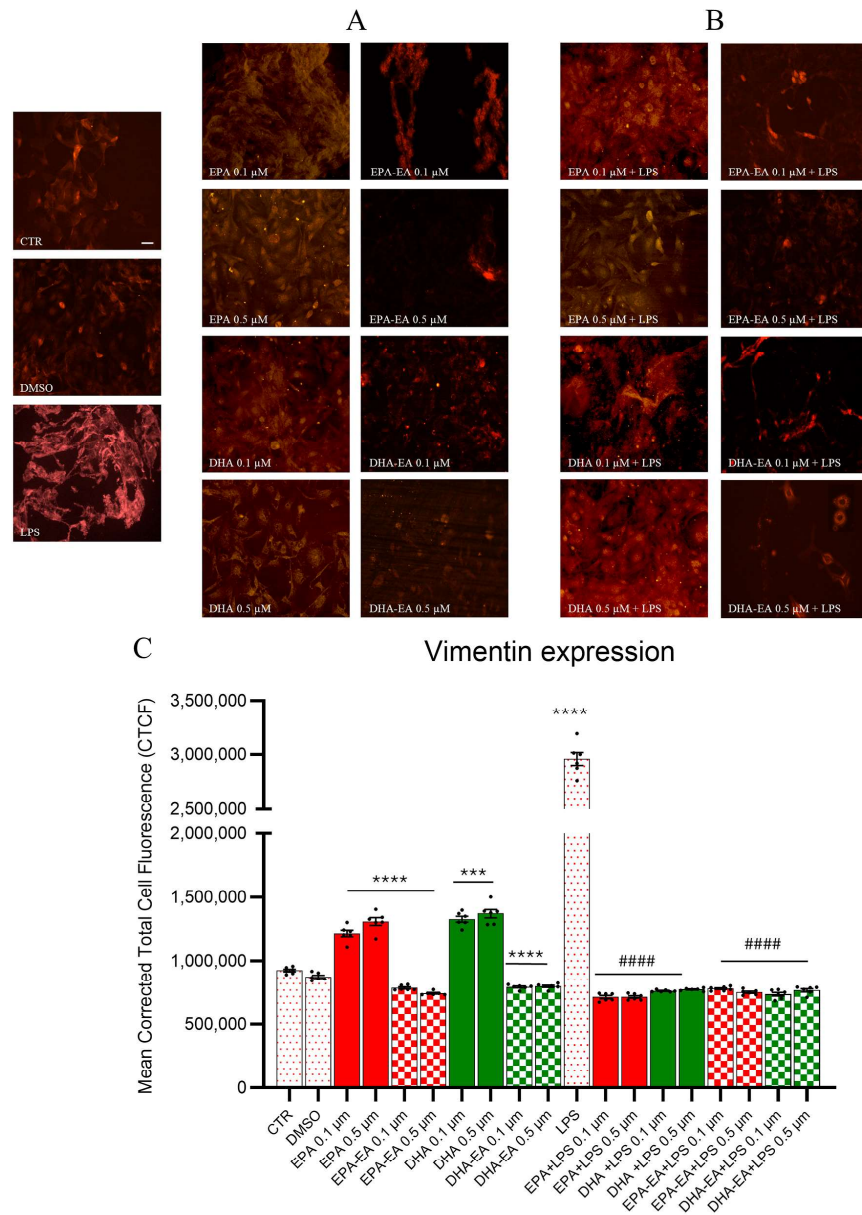


Figure 8. Immunocytochemistry for vimentin in OECs exposed to different treatments. The test was carried out on OECs without (A) and with (B) LPS exposure and treated with EPA, DHA, EPA-EA, and DHA-EA. (C) Fluorescence quantification data for vimentin in each OEC treatment with EPA, DHA, EPA-EA, and DHA-EA at different concentrations (0.1 μm and 0.5 μm). Bars represent CTCF mean value ± SD, obtained from at least three independent experiments. One-way ANOVA experimental groups vs. CTR, $F(18, 95) = 375.5$. One-way ANOVA experimental groups vs. LPS, $F(16, 85) = 396.1$. Dunnett’s multiple comparison test: *** $p < 0.001$; **** $p < 0.0001$ vs. CTR; #### $p < 0.0001$ vs. LPS. Scale bar 20 μm.

From images shown in Figures 7B and 8B and the corresponding histograms for fluorescence quantification (Figures 7C and 8C), it can be evidenced that the positivity of GFAP and vimentin in OECs cells, as such or exposed to LPS, treated with EPA-EA and DHA-EA was lower compared to that observed for EPA and DHA.

3. Discussion

In this study we investigated, for the first time, the role of EPA and DHA and corresponding *N*-ethanolamides EPA-EA and DHA-EA in OECs exposed to stress of LPS for 24 h and reported their protective activity against cell death and inflammation.

Several works have reported that PUFA is essential for the normal development of the central nervous system and for neural stem cell differentiation [43]. In particular, DHA plays a role in neuropsychiatric disorders, such as depression or dementia [44], and it has been demonstrated that PUFA deficiency can affect cerebral functions and alter the development of the brain, involving the membranes of neurons, oligodendrocytes, and astrocytes [12].

In this study, we chose to use mouse primary cultures of OECs, a particular glial cell type located in the olfactory system, as a useful experimental model for neuroinflammation after exposing them to LPS to induce an inflammatory event. Due to their peculiar characteristics, in recent years, OECs have attracted interest for their use in cell therapy [33,35,45], and LPS is considered an effective insult for inflammatory induction in neural cells. The concentrations of the compounds and DMSO used in all the experiments were preliminarily assessed as not toxic for the cells.

The evaluation of protective effects exerted by EPA, DHA, and the related ethanolamides EPA-EA and DHA-EA on viability and cellular morphology of OECs exposed to LPS-induced inflammation was carried out by both toxicity and immunocytochemistry assays.

Results from MTT, MitoHealth, and TUNEL assays all evidenced, for the first time, the efficacy of the tested compounds in improving OEC viability and contrasting the cytotoxic effect exerted by LPS on these cells. A similar protective effect had also been observed in a model set up with differentiated SH-SY5Y cells exposed to A β 25–35 [46]. More in detail, we found that EPA exerts greater protection than DHA on OECs exposed to LPS, in agreement with data reported by Ceccarini et al. [14] that demonstrated that EPA, but not DHA, reduces the toxic effect exerted by neurotoxin 6-hydroxydopamine (6-OHDA) in SH-SY5Y cell line, through increase BDNF and GDNF levels via epigenetic mechanisms.

Apoptosis has been found to be responsible for pathological conditions for the loss of neurons in several neurodegenerative diseases, such as Parkinson's disease, Alzheimer's disease, amyotrophic lateral sclerosis, and aging. Brains of patients suffering neurodegenerative diseases have shown significant DNA fragmentation detected by the TUNEL test, reduced expression of anti-apoptotic Bcl-2, and the presence of activated caspase-3 in neurons, so demonstrating the involvement of apoptosis in the pathogenesis of neurodegenerative diseases [47]. Mitochondrial fragmentation induced by the expression of caspase-3-cleaved tau sensitizes mitochondria to a neurotoxic effect associated with Alzheimer's disease [48]. Furthermore, the role of mitochondria, in addition to providing energy through ATP, is to regulate cell calcium activity, which is essential for neurotransmitter release [49]. Thus, we decided to highlight the potential protective role of the target compounds by monitoring their efficacy in reducing apoptosis and improving the mitochondrial health of LPS-exposed OECs.

The obtained results by MitoHealth and TUNEL assays for EPA and DHA (both acids and amides) on OECs suggest a beneficial effect of the tested compounds in controlling effects of inflammation and in preventing the onset of neurodegenerative diseases through a reduction in mitochondrial fragmentation and apoptosis, in agreement with Eckert et al. [50].

Some authors report that cytoskeleton proteins, such as vimentin and GFAP, are involved in several cellular functions and in stress conditions, so their expression is considered a biomarker of astrocyte activation and astrogliosis caused by lesions or neurodegenerative diseases [51,52]. Therefore, in order to gain better evidence of the anti-inflammatory activity of the tested compounds, immunocytochemistry assays targeted to the quantification of the expression levels of specific proteins related to inflammation

were carried out, and among the possible proteins, we considered two cytoskeleton proteins, vimentin and GFAP, and the cytokine IL-10. Cytoskeleton changes, indeed, are involved in the pathogenesis of some neurodegenerative diseases, and morphological features resulting from increased glial reactivity in OECs exposed to LPS and treated with the compounds in hands were monitored through the expression of cytoskeleton markers, which play an important role in astrogliosis, a typical sign of an inflammation event [53].

The treatment of LPS-stressed OECs with EPA, DHA, EPA-EA, and DHA-EA resulted in the same protein expression levels compared to the control, or even lower in the case of GFAP, evidencing an anti-inflammatory activity of these compounds. The decreased GFAP and vimentin expression, indeed, indicated a decrease in reactive LPS-induced astrogliosis and highlighted the protective effect of EPA-EA and DHA-EA on OECs.

The obtained results are in agreement with a study conducted by Tyrtysnaia et al. [54], in which the authors reported that both EPA-EA and DHA-EA counteract the LPS-mediated increase in GFAP expression, with a superior anti-inflammatory activity found for DHA-EA compared to EPA-EA in vitro and in vivo studies. The lower EPA-EA activity might be due to a lower content of this molecule within the brain compared with DHA-EA [25].

Other support for the anti-inflammatory activity of the tested compounds on OECs comes from the evaluation of levels of IL-10, one among many cytokines produced by LPS induction. While a strong positivity to IL-10 was found in OECs exposed to LPS, levels of IL-10 in treated cells were reduced as in the control.

These obtained data suggest a structure-related activity, with EPA and DHA predominantly exerting a protective role on cell morphology and viability, as deduced by monitoring obtained from the inverted microscope as well as MTT, TUNEL, and DeadGreen staining in the MitoHealth test, while amides EPA-EA and DHA-EA mainly show anti-inflammatory effects superior to those of free acids due to their ability to better suppress the expression of cytoskeleton proteins and the cytokine IL-10 in LPS-stressed OECs.

Concentration levels of DHA-EA and EPA-EA are related to those of DHA and EPA and have been shown to increase after consumption of a fish oil-rich or DHA-supplemented diet [55]. Therefore, the administration of a DHA/EPA diet could counteract neuroinflammation effects and improve cognitive activities, preventing the decline associated with aging in humans.

4. Materials and Methods

4.1. Reagents

(5Z,8Z,11Z,14Z,17Z)-Eicosapentenoic acid (EPA), (4Z,7Z,10Z,13Z,16Z,19Z)-docosahexaenoic acid (DHA), and ethanolamine were purchased from Sigma-Aldrich (St. Louis, MO, USA) and used as received. The corresponding ethyl esters EPA-EE and DHA-EE were obtained from Solutex (Madrid, Spain). Immobilized lipase from *Candida antarctica* (Novozym® 435) was obtained from Strem Chemicals Inc. (Newburyport, MA, USA). Additionally, 3 Å Molecular sieves (Aldrich, St. Louis, MO, USA) were activated by heating at 100 °C for 3 h before use. Lipopolysaccharide (LPS) was obtained from Santa Cruz (Dallas, TX, USA, sc-3535) and dissolved in sterile PBS.

4.2. Synthesis of EPA-EA and DHA-EA

The synthesis of title compounds was carried out as previously reported [42]. Briefly, to a solution of EPA-EE or DHA-EE (200 mg) in tert-butyl methyl ether (6 mL), Novozym® 435 (100 mg), molecular sieves (100 mg), and ethanolamine (1.1 eqv.) were added, and the suspension stirred in a shaker at 45 °C for 12–24 h. At the end of the reaction, as stated by TLC analysis (*n*-hexane/EtOAc 9:1), the mixture was extracted with 2 M HCl, and the organic phase was separated. The organic solvent was removed under reduced pressure,

and the products EPA-EA or DHA-EA were recovered as pale-yellow oils in 90–95% yield. Further purification was carried out by column chromatography on Si gel, eluting with *n*-hexane/EtOAc 1:1 containing 5% EtOH *v/v*. ¹H- and ¹³C-NMR spectra were registered on a Bruker Avance TM 400 spectrometer (Bruker Milano, Milan, Italy) at 400.13 and 100.62 MHz, respectively, and were found in agreement with those reported. Chemical purity (>98%) was checked by HPLC on a SphereClone Silica 80 Å (Phenomenex, Inc. Bologna, Italy) column (250 × 4.6 mm, 5 µm) eluting with *n*-hexane:2-PrOH 85:15 mixture at flow 0.5 mL/min and using UV-detection at 220 nm.

4.3. OEC Cultures

OECs were obtained from 2-day-old mouse pups (P2) olfactory bulbs (Envigo RMS s.r.l., Udine, Italy). All the experiments were carried out according to the Italian Guidelines for Animal Care (D.L. 116/92 and 26/2014), which are in compliance with the European Communities Council Directives (2010/63/EU) and approved by the Ethical Committee at the Catania University (Italy) and National Ministry of Health (permit number 174/2017-PR).

Olfactory bulbs were digested in MEM-H, containing a collagenase and trypsin mixture as previously described [56]. Trypsinization was stopped by adding DMEM supplemented with 10% FBS (DMEM/FBS, GIBCO, Waltham, MA, USA). Cells were re-suspended and plated in flasks fed with complete DMEM/FBS. An antimetabolic agent, cytosine arabinoside (10–5 M), was added 24 h after initial plating to reduce the number of dividing fibroblasts. When OECs were confluent, they were removed by trypsin, transferred on 25 cm² flasks, cultured in DMEM/FBS, and incubated at 37 °C in a humidified 5% CO₂–95% air mixture.

4.4. Treatment of Cells

Purified OECs were grown in DMEM/FBS on both 13 mm diameter glass coverslips and 96-multi-wells plates and incubated at 37 °C in a humidified 5% CO₂–95% air mixture. In preliminary experiments, we screened different concentrations (0.1, 0.25, 0.5, and 5 µM) of target compounds and LPS (10 and 20 µg/mL) in order to establish non-toxic concentrations. Working concentrations of target compounds were set at 0.1 and 0.5 µM, and no difference was found at higher concentrations (by MTT assay). The optimal time of exposure of OECs to LPS and to the target compounds was set to 24 h, chosen according to our previous study [57]. OEC cultures were divided into different groups: as controls, we considered (1) a group contained only OECs, (2) a group treated with DMSO (0.008% *v/v*), the solvent used to solubilize the tested compounds, and (3) a group stressed for 24 h with LPS (10 µg/mL) [58]. In addition, we set up: (4) two groups treated with EPA 0.1 µM or 0.5 µM for 24 h; (5) two other groups treated with DHA 0.1 µM or 0.5 µM for 24 h; (6) two groups treated with EPA-EA 0.1 µM or 0.5 µM for 24 h; (7) other two groups treated with DHA-EA 0.1 µM or 0.5 µM for 24 h. Four other groups were the same as groups 4–7 with the addition of LPS.

Possible changes in cellular morphology were qualitatively evaluated after 24 h by phase-contrast inverted microscopy (AXIOVERT 100, Zeiss, Jena, Germany), capturing the images with the Axiovision imaging system. For the following experiments, no a priori sample size calculation was performed, and all experiments were performed in a non-blinded manner.

4.5. MTT Assay

Cellular viability was assessed through an MTT test [56] on OECs grown into 96-multi-well plates. In detail, 3-[4,5-dimethylthiazol-2-yl]2,5-diphenyl]tetrazolium bromide (MTT; Sigma, Kawasaki, Japan) was added to each multi-well at a final concentration of 1.0 mg/mL and incubated for 2 h in a CO₂ incubator. Subsequently, isopropanol/SDS, an MTT solvent, was added, and cells were agitated on an orbital shaker

for 15 min. The optical density was evaluated at $\lambda = 570$ nm with a microplate spectrophotometer reader (Cary 50 MPR microplate reader—Varian© 237, Palo Alto, CA, USA). Four replicates were carried out for each experimental condition, and results were expressed as the percentage MTT reduction in the control cells.

4.6. TUNEL (Terminal Deoxynucleotidyl Transferase dUTP Nick End Labeling) Test

Dead cells were counted by staining with the Click-iT™ TUNEL Alexa Fluor™ 488 Imaging assay (Thermo Fisher Scientific© Waltham, MA, USA), based on the incorporation of the modified nucleotide deoxyuridine triphosphate (dUTPs) at the 3'-OH ends of fragmented DNA by the enzyme terminal deoxynucleotidyl transferase (TdT). OECs were cultured on glass coverslips and exposed to LPS in the presence of EPA, DHA, EPA-EA, and DHA-EA for 24 h. Cells were fixed with 4% PFA, permeabilized with 0.25% Triton X-100, and processed following the manufacturing instructions. Coverslips were scanned with a Nikon Ti-Eclipse inverted microscope (Nikon©, Tokyo, Japan) equipped with a Plan Aplanachromat lambda 60×/1.4 oil immersion lens (Nikon©, Tokyo, Japan) and data acquired with NIS-Elements AR (Advanced Research) software (version 4.60) (Nikon©, Tokyo, Japan). TUNEL-positive cells were counted with the “CellCount” option in the NIS-Elements AR v4.60 software (Nikon, Tokyo, Japan), adjusting pixel threshold, size, and circularity, and reported as TUNEL+ nuclei/total cell number (DAPI+ nuclei) × 100 [59].

4.7. Mitochondrial Health Assay

Mitotoxicity and cytotoxicity in all OEC experimental conditions were detected by using the HCS Mitochondrial Health Kit (Thermo Fisher Scientific©, Waltham, MA, USA). Cells were plated into glass coverslips and exposed to LPS in the presence of EPA, DHA, EPA-EA, and DHA-EA for 24 h (three glass coverslips were carried out for each experimental condition). Briefly, following manufacture instructions, cells were incubated for 30 min with MitoHealth reagent, which accumulates in the mitochondria of living cells proportionally to the mitochondrial membrane potential, and with Image-iT DEAD™ Green™ stain, an impermeant dye to healthy cells that forms highly fluorescent dye-DNA complexes if plasma membrane integrity is compromised. Then, OECs were washed with PBS and fixed with 4% paraformaldehyde (PFA); the blue-fluorescent dye nuclear segmentation 4',6-diamidino-2-phenylindole (DAPI) (Thermo Fisher Scientific©, Waltham, Massachusetts, USA) was used to visualize the nuclear compartment. Coverslips were visualized with a Nikon Ti-Eclipse inverted microscope through a Plan Aplanachromat Lambda 60×/1.4 oil immersion lens (Nikon©, Tokyo, Japan), and images were acquired with NIS-Elements AR v4.60 software (Nikon©, Tokyo, Japan). The fluorescence was quantified by analyzing the mean intensity of each channel from at least ten multiple regions of interest (ROI) normalized to the background by using the NIS-Elements AR (Advanced Research) software (version 4.60), as previously described by La Cognata et al. [59].

4.8. Immunocytochemistry

Immunocytochemical procedures to detect the expression of IL-10, an inflammation marker, vimentin, and GFAP, both cytoskeleton proteins, were applied to the cells incubated for 24 h in all the different experimental conditions. Cells were fixed by 4% PFA in 0.1 M phosphate-buffered saline (PBS) for 30 min. After washing in PBS, the cell membranes were permeabilized with 5% normal goat serum (NGS) in PBS containing 0.1% Triton X-100 (PBS-Triton) at room temperature for 15 min and then incubated overnight at 4 °C with the following primary antibodies: polyclonal antibody anti-IL10 (1:400, AbCAM, Waltham, MA, USA), mouse monoclonal antibody against vimentin (1:50, DAKO M0725, Santa Clara, CA, USA), and polyclonal antibody against GFAP (1:1000, DAKO, Z0334, Santa Clara, CA, USA). Secondary antibodies Cy3 anti-rabbit and

Cy3 anti-mouse (1:500, Jackson Immunoresearch, Cambridge, UK) were used to visualize IL-10 and vimentin antibodies, respectively. Fluorescein Isothiocyanate (FITC)-conjugated goat anti-rabbit IgG antibody (diluted 1:200; Jackson Immunological Research Laboratories Inc., West Grove, PA, USA) was used to visualize GFAP antibody. OECs were incubated with the secondary antibodies for 1 h at room temperature and in dark conditions. The immunostained coverslips were analyzed with a fluorescence microscope (Carl Zeiss©, Jena, Germany), and images were captured with the Axiovision imaging system (Zen3.6-Blue edition). In all cell cultures in which primary antibodies were omitted, no specific staining was observed.

4.9. Immunostaining Quantification

The FIJI-ImageJ (1.52v software) measure tool (NIH, Bethesda, MD, USA) was used to carry out the immunostaining quantification. From each group, at least three samples were investigated at each time point. From each sample, three digital photomicrographs were randomly selected, and from each one, up to seven immunofluorescent cells were analyzed. Values were derived from the average grayscale intensity. The integrated density, the cell area, and the mean fluorescence of the selected cells were evaluated. At least three replicate measurements were performed for each capture region. The same procedure was applied to three different background areas around the selected cell. Then, the Corrected Total Cell Fluorescence (CTCF) was calculated using the following equation: $CTCF = \text{integrated density} (\text{cell area} \times \text{background mean fluorescence})$.

4.10. Statistical Analysis

All experiments were repeated, at least in triplicate. Statistical analysis was performed using GraphPad Prism 9.0 (GraphPad Software, La Jolla, CA, USA). For immunofluorescence experiments, CTCF values are reported as mean \pm SD. For TUNEL and MitoHealth/Dead green staining, values are reported as mean \pm SEM. Differences between samples were assessed using a One-way analysis of variance (One-way ANOVA) followed by a post hoc Dunnett's test. Significance was defined as follows: ** $p < 0.01$; *** $p < 0.001$; **** $p < 0.0001$ vs. CTR; # $p < 0.05$; ## $p < 0.01$; ### $p < 0.001$; #### $p < 0.0001$ vs. LPS.

5. Conclusions

In this study, a comparative analysis of the anti-inflammatory effects of EPA, DHA, and the corresponding *N*-ethanolamides in two different concentrations on typical olfactory glial cells, OECs, exposed to LPS-induced inflammation was reported.

Our results show that all the tested compounds are neither cytotoxic nor mitotoxic at the tested concentrations. Indeed, the amide derivatives stimulate mitochondrial activity with an improvement in their metabolism. They also exert protective effects on OECs exposed to LPS by slowing down the cell death progression, reducing the expression of the IL-10 cytokine, and avoiding LPS-induced astrogliosis, as deduced by the decrease in the expression of cytoskeleton proteins such as GFAP and vimentin. All these data would contribute to attributing significant anti-inflammatory and neuroprotective activity to all the tested compounds, even if a more pronounced suppression of the inflammatory event was found for DHA-EA at both concentrations compared to EPA-EA in OECs exposed to LPS.

In conclusion, our results, with the limitations associated with *in vitro* rather than *in vivo* experiments, highlight that EPA and DHA, both as free acids and *N*-ethanolamide derivatives, show high therapeutic potential in slowing the onset of the neurodegenerative diseases, so opening new prospects for therapeutic strategies. As a perspective in our future investigation, the protective role of the compounds here investigated against LPS-induced neuroinflammation would deserve a more in-depth study on olfactory glia cells in an *in vivo* model.

Author Contributions: Conceptualization, A.P., C.S. and R.P.; methodology, C.S. and R.P.; software, V.L.C. and C.R.; validation, A.P., C.S. and R.P.; formal analysis, V.L.C. and C.R.; investigation, C.S. and R.P.; resources, C.S. and R.P.; data curation, A.P., C.S. and R.P.; writing—original draft preparation, A.P. and R.P.; writing—review and editing, A.P. and R.P.; visualization, A.P., C.S. and R.P.; supervision, A.P. and R.P.; project administration, R.P.; funding acquisition, R.P. All authors have read and agreed to the published version of the manuscript.

Funding: This research was funded by Progetto NUTRAGE (FOE 2021)—DM MUR n. 844 del 16/07/2021—CUP B83C21001810005 (DBA.AD005.225).

Institutional Review Board Statement: Not applicable.

Informed Consent Statement: Not applicable.

Data Availability Statement: The data presented in this study are available in the article.

Acknowledgments: The authors wish to thank Francesco Marino (IRIB-CNR, Catania) for his helpful work with figure editing.

Conflicts of Interest: The authors declare no conflicts of interest.

References

1. Zhu, Y.; Chen, X.; Liu, Z.; Peng, Y.P.; Qiu, Y.H. Interleukin-10 protection against lipopolysaccharide-induced neuroinflammation and neurotoxicity in ventral mesencephalic cultures. *Int. J. Mol. Sci.* **2016**, *17*, 25.
2. Lucin, K.M.; Wyss-Coray, T. Immune activation in brain aging and neurodegeneration: Too much or too little? *Neuron* **2009**, *64*, 110–122.
3. Bartels, T.; De Schepper, S.; Hong, S. Microglia modulate neurodegeneration in Alzheimer's and Parkinson's diseases. *Science* **2020**, *370*, 66–69.
4. Shao, F.; Wang, X.; Wu, H.; Wu, Q.; Zhang, J. Microglia and neuroinflammation: Crucial pathological mechanisms in traumatic brain injury-induced neurodegeneration. *Front. Aging Neurosci.* **2022**, *14*, 825086.
5. Paterniti, I.; Impellizzeri, D.; Di Paola, R.; Esposito, E.; Gladman, S.; Yip, P.; Priestley, J.V.; Michael-Titus, A.T.; Cuzzocrea, S. Docosahexaenoic acid attenuates the early inflammatory response following spinal cord injury in mice: In-vivo and in-vitro studies. *J. Neuroinflamm.* **2014**, *11*, 6.
6. Guo, S.; Wang, H.; Yin, Y. Microglia polarization from M1 to M2 in neurodegenerative diseases. *Front. Aging Neurosci.* **2022**, *14*, 815347.
7. Aldana, B.I. Microglia-specific metabolic changes in neurodegeneration. *J. Mol. Biol.* **2019**, *431*, 1830–1842.
8. Yang, C.; Pan, R.Y.; Guan, F.; Yuan, Z. Lactate metabolism in neurodegenerative diseases. *Regen. Res.* **2024**, *19*, 69–74.
9. Woodburn, S.C.; Bollinger, J.L.; Wohleb, E.S. The semantics of microglia activation: Neuroinflammation; homeostasis; and stress. *J. Neuroinflamm.* **2021**, *18*, 258.
10. Stillwell, W.; Wassall, S.R. Docosahexaenoic acid: Membrane properties of a unique fatty acid. *Chem. Phys. Lipids* **2003**, *126*, 1–27.
11. Petermann, A.B.; Reyna-Jeldes, M.; Ortega, L.; Coddou, C.; Yévenes, G.E. Roles of the unsaturated fatty acid docosahexaenoic acid in the central nervous system: Molecular and cellular insights. *Int. J. Mol. Sci.* **2022**, *23*, 5390.
12. Bourre, J. Roles of unsaturated fatty acids (especially omega-3 fatty acids) in the brain at various ages and during ageing. *J. Nutr. Health Aging* **2004**, *8*, 163–174.
13. Dyall, S.C. Long-chain omega-3 fatty acids and the brain: A review of the independent and shared effects of EPA; DPA and DHA. *Front. Aging Neurosci.* **2015**, *7*, 52.
14. Ceccarini, M.R.; Ceccarelli, V.; Codini, M.; Fettucciari, K.; Calvitti, M.; Cataldi, S.; Albi, E.; Vecchini, A.; Beccari, T. The polyunsaturated fatty acid EPA; but not DHA; enhances neurotrophic factor expression through epigenetic mechanisms and protects against parkinsonian neuronal cell death. *Int. J. Mol. Sci.* **2022**, *23*, 16176.
15. Park, H.; Poo, M.M. Neurotrophin regulation of neural circuit development and function. *Nat. Rev. Neurosci.* **2013**, *14*, 7–23.
16. Rahman, M.M.; Islam, M.R.; Supti, F.A.; Dhar, P.S.; Shohag, S.; Ferdous, J.; Shuvo, S.K.; Akter, A.; Hossain, M.S.; Sharma, R. Exploring the therapeutic effect of neurotrophins and neuropeptides in neurodegenerative diseases: At a glance. *Mol. Neurobiol.* **2023**, *60*, 4206–4231.
17. Kawakita, E.; Hashimoto, M.; Shido, O. Docosahexaenoic acid promotes neurogenesis in vitro and in vivo. *Neuroscience* **2006**, *139*, 991–997.
18. Chapkin, R.S.; Kim, W.; Lupton, J.R.; McMurray, D.N. Dietary docosahexaenoic and eicosapentaenoic acid; Emerging mediators of inflammation. *Prostaglandins Leukot. Essent. Fatty Acids* **2009**, *81*, 187–191.
19. Layé, S.; Nadjar, A.; Joffre, C.; Bazinet, R.P. Anti-inflammatory effects of omega-3 fatty acids in the brain: Physiological mechanisms and relevance to pharmacology. *Pharmacol. Rev.* **2018**, *70*, 12–38.
20. Moon, D.O.; Kim, K.C.; Jin, C.Y.; Han, M.H.; Park, C.; Lee, K.J.; Park, Y.M.; Choi, Y.H.; Kim, G.Y. Inhibitory effects of eicosapentaenoic acid on lipopolysaccharide-induced activation in BV2 microglia. *Int. Immunopharmacol.* **2007**, *7*, 222–229.

21. Liuzzi, G.M.; Latronico, T.; Rossano, R.; Viggiani, S.; Fasano, A.; Riccio, P. Inhibitory effect of polyunsaturated fatty acids on MMP-9 release from microglial cells—implications for complementary multiple sclerosis treatment. *Neurochem. Res.* **2007**, *32*, 2184–2193.
22. De Smedt-Peyrusse, V.; Sargueil, F.; Moranis, A.; Harizi, H.; Mongrand, S.; Layé, S. Docosahexaenoic acid prevents lipopolysaccharide-induced cytokine production in microglial cells by inhibiting lipopolysaccharide receptor presentation but not its membrane subdomain localization. *J. Neurochem.* **2008**, *105*, 296–307.
23. Serhan, C.N.; Dalli, J.; Colas, R.A.; Winkler, J.W.; Chiang, N. Protectins and maresins: New pro-resolving families of mediators in acute inflammation and resolution bioactive metabolome. *Biochim. Biophys. Acta* **2015**, *1851*, 397–413.
24. Serhan, C.N.; Levy, B.D. Resolvins in inflammation: Emergence of the pro-resolving superfamily of mediators. *J. Clin. Investig.* **2018**, *128*, 2657–2669.
25. Meijerink, J.; Balvers, M.; Witkamp, R. N-Acyl amines of docosahexaenoic acid and other n-3 polyunsaturated fatty acids: From fishy endocannabinoids to potential leads. *Br. J. Pharmacol.* **2013**, *169*, 772–783.
26. Park, T.; Chen, H.; Kevala, K.; Lee, J.W.; Kim, H.Y. N-Docosahexaenoylethanolamine ameliorates LPS-induced neuroinflammation via cAMP/PKA-dependent signaling. *J. Neuroinflamm.* **2016**, *13*, 284.
27. Fairless, R.; Barnett, S. Olfactory ensheathing cells: Their role in central nervous system repair. *Int. J. Biochem. Cell. Biol.* **2005**, *37*, 693–699.
28. Graziadei, P.P.C.; Monti-Graziadei, G.A. Neurogenesis and neuron regeneration in the olfactory system of mammals. I. Morphological aspects of differentiation and structural organization of the olfactory sensory neurons. *J. Neurocytol.* **1979**, *8*, 1–18.
29. Pellitteri, R.; Spatuzza, M.; Stanzani, S.; Zaccheo, D. Biomarkers expression in rat olfactory ensheathing cells. *Front. Biosci.* **2010**, *2*, 289–298.
30. Lipson, A.C.; Widenfalk, J.; Lindqvist, E.; Ebendal, T.; Olson, L. Neurotrophic properties of olfactory ensheathing glia. *Exp. Neurol.* **2003**, *180*, 167–171.
31. Pastrana, E.; Moreno-Flores, M.T.; Avila, J.; Wandosel, F.; Minichiello, L.; Diaz-Nido, J. BDNF production by olfactory ensheathing cells contributes to axonal regeneration of cultured adult CNS neurons. *Neurochem. Int.* **2007**, *50*, 491–498.
32. Doucette, R. Immunohistochemical localization of laminin; fibronectin and collagen type IV in the nerve fiber layer of the olfactory bulb. *Int. J. Dev. Neurosci.* **1996**, *14*, 945–959.
33. Ramon-Cueto, A.; Avila, J. Olfactory ensheathing cells: Properties and function. *Brain Res. Bull.* **1998**, *46*, 175–177.
34. Franssen, E.H.; de Bree, F.M.; Verhaagen, J. Olfactory ensheathing glia: Their contribution to primary olfactory nervous system regeneration and their regenerative potential following transplantation into the injured spinal cord. *Brain Res. Rev.* **2007**, *56*, 236–258.
35. Pellitteri, R.; Cova, L.; Zaccheo, D.; Silani, V.; Bossolasco, P. Phenotypic modulation and neuroprotective effects of olfactory ensheathing cells: A promising tool for cell therapy. *Stem Cell Rev. Rep.* **2016**, *12*, 224–234.
36. Delarue, Q.; Guérout, N. Transplantation of Olfactory Ensheathing Cells: Properties and therapeutic effects after transplantation into the lesioned nervous system. *Neuroglia* **2022**, *3*, 1–22.
37. Nazareth, L.; Lineburg, K.E.; Chuah, M.I.; Velasquez, J.T.; Chehrehasa, F.; John, J.S.; Ekberg, J.A. Olfactory ensheathing cells are the main phagocytic cells that remove axon debris during early development of the olfactory system. *J. Comp. Neurol.* **2015**, *523*, 479–494.
38. Nazareth, L.; Shelper, T.B.; Chacko, A.; Basu, S.; Delbaz, A.; Lee, J.Y.P.; Chen, M.; John, J.A.S.; Ekberg, J.A.K. Key differences between olfactory ensheathing cells and Schwann cells regarding phagocytosis of necrotic cells: Implications for transplantation therapies. *Sci. Rep.* **2020**, *10*, 18936.
39. Russo, C.; Patané, M.; Vicario, N.; Di Bella, V.; Cosentini, I.; Barresi, V.; Gulino, R.; Pellitteri, R.; Russo, A.; Stanzani, S. Olfactory ensheathing cells express both ghrelin and ghrelin receptor in vitro: A new hypothesis in favor of a neurotrophic effect. *Neuropeptides* **2020**, *79*, 101997.
40. Erekat, N.S. Apoptosis and its therapeutic implications in neurodegenerative diseases. *Clin. Anat.* **2022**, *35*, 65–78.
41. Qin, L.; Wu, X.; Block, M.L.; Liu, Y.; Breese, G.R.; Hong, J.S.; Knapp, D.; Crews, F.T. Systemic LPS causes chronic neuroinflammation and progressive neurodegeneration. *Glia* **2007**, *55*, 453–462.
42. Sanfilippo, C.; Patti, A. Biocatalytic regio- and stereoselective access to ω -3 endocannabinoid epoxides with peroxygenase from oat flour. *Bioorg. Chem.* **2021**, *113*, 105014.
43. Katakura, M.; Hashimoto, M.; Okui, T.; Shahdat, H.M.; Matsuzaki, K.; Shido, O. Omega-3 polyunsaturated-fatty acids enhance neuronal differentiation in cultured rat neural stem cells. *Stem Cells Int.* **2013**, *2013*, 490476.
44. Mazza, M.; Pomponi, M.; Janiri, L.; Bria, P.; Mazza, S. Omega-3 fatty acids and antioxidants in neurological and psychiatric diseases: An overview. *Prog. Neuro-Psychopharmacol. Biol. Psychiatry* **2006**, *31*, 12–26.
45. Zhang, L.P.; Liao, J.X.; Liu, Y.Y.; Luo, H.L.; Zhang, W.J. Potential therapeutic effect of olfactory ensheathing cells in neurological diseases: Neurodegenerative diseases and peripheral nerve injuries. *Front. Immunol.* **2023**, *14*, 1280186.
46. Zhang, Y.P.; Brown, R.E.; Zhang, P.C.; Zhao, Y.T.; Ju, X.; Song, C. DHA, EPA and their combination at various ratios differently modulated A β 25-35-induced neurotoxicity in SH-SY5Y cells. *Prostaglandins Leukot. Essent. Fatty Acids* **2018**, *136*, 85–94.
47. Park, G.; Nhan, H.S.; Tyan, S.H.; Kawakatsu, Y.; Zhang, C.; Navarro, M.; Koo, E.H. Caspase activation and caspase-mediated cleavage of APP is associated with amyloid beta-protein-induced synapse loss in Alzheimer's disease. *Cell Rep.* **2020**, *31*, 107839.

48. Perez, M.J.; Ibarra-García-Padilla, R.; Tang, M.; Porter, J.A., Jr.; Johnson, G.V.W.; Quintanilla, R.A. Caspase-3 cleaved tau impairs mitochondrial function through the opening of the mitochondrial permeability transition pore. *Biochim. Biophys. Acta Mol. Basis Dis.* **2024**, *1870*, 166898.
49. Gendron, T.F.; Petrucelli, L. The role of tau in neurodegeneration. *Mol. Neurodegener.* **2009**, *4*, 13.
50. Eckert, G.P.; Lipka, U.; Muller, W.E. Omega-3 fatty acids in neurodegenerative diseases: Focus on mitochondria. *Prostaglandins Leukot. Essent. Fatty Acids* **2013**, *88*, 105–114.
51. Lee, S.Y.; Surbeck, J.W.; Drake, M.; Saunders, A.; Jin, H.D.; Shah, V.A.; Rajala R.V. Increased glial fibrillary acid protein and vimentin in vitreous fluid as a biomarker for proliferative vitreoretinopathy. *Investig. Ophthalmol. Vis. Sci.* **2020**, *61*, 22.
52. Wilhelmsson, U.; Pozo-Rodríguez, A.; Kalm, M.; de Pablo, Y.; Widestrand, Å.; Pekna, M.; Pekny, M. The role of GFAP and vimentin in learning and memory. *Biol. Chem.* **2019**, *400*, 1147–1156.
53. Osborn, L.M.; Kamphuis, W.; Wadman, W.J.; Hol, E.M. Astrogliosis: An integral player in the pathogenesis of Alzheimer's disease. *Prog. Neurobiol.* **2016**, *144*, 121–141.
54. Tyrtysnaia, A.; Konovalova, S.; Bondar, A.; Ermolenko, E.; Sultanov, R.; Manzhulo, I. Anti-inflammatory activity of N-docosahexaenylethanolamine and N-eicosapentaenylethanolamine in a mouse model of lipopolysaccharide-induced neuroinflammation. *Int. J. Mol. Sci.* **2021**, *22*, 10728.
55. Joffre, C.; Dinel, A.L.; Chataigner, M.; Pallet, V.; Layé, S. n-3 Polyunsaturated Fatty Acids and Their Derivates Reduce Neuroinflammation during Aging. *Nutrients* **2020**, *12*, 647.
56. Pellitteri, R.; Catania, M.V.; Bonaccorso, C.M.; Ranno, E.; Dell'Albani, P.; Zaccheo, D. Viability of olfactory ensheathing cells after hypoxia and serum deprivation: Implication for therapeutic transplantation: Role of Growth Factors in Hypoxic OECs. *J. Neurosci. Res.* **2014**, *92*, 1757–1766.
57. Campisi, A.; Spatuzza, M.; Russo, A.; Raciti, G.; Vanella, A.; Stanzani, S.; Pellitteri, R. Expression of Tissue Transglutaminase on Primary Olfactory Ensheathing Cells Cultures Exposed to Stress Conditions. *Neurosci. Res.* **2012**, *72*, 289–295.
58. Li, H.; Huynh, T.N.; Duong, M.T.; Gow, J.G.; Chang, C.C.Y.; Chang, T.Y. ACAT1/SOAT1 Blockade Suppresses LPS-Mediated Neuroinflammation by Modulating the Fate of Toll-like Receptor 4 in Microglia. *Int. J. Mol. Sci.* **2023**, *24*, 5616.
59. La Cognata, V.; Golini, E.; Iemmolo, R.; Balletta, S.; Morello, G.; De Rosa, C.; Villari, A.; Marinelli, S.; Vacca, V.; Bonaventura, G.; et al. CXCR2 increases in ALS cortical neurons and its inhibition prevents motor neuron degeneration in vitro and improves neuromuscular function in SOD1G93A mice. *Neurobiol. Dis.* **2021**, *160*, 105538.

Disclaimer/Publisher's Note: The statements, opinions and data contained in all publications are solely those of the individual author(s) and contributor(s) and not of MDPI and/or the editor(s). MDPI and/or the editor(s) disclaim responsibility for any injury to people or property resulting from any ideas, methods, instructions or products referred to in the content.